

# Characteristics of the cloud enhancement phenomenon and PV power plants

Markku Järvelä\*, Kari Lappalainen, Seppo Valkealahti

Tampere University, Electrical Engineering, P.O. Box 692, FI-33101 Tampere, Finland

## ARTICLE INFO

### Keywords:

Cloud enhancement  
PV generator  
Irradiance enhancement  
Renewables integration

## ABSTRACT

The cloud enhancement (CE) of solar irradiance is a well-known phenomenon, but its effects on PV power plants are not thoroughly understood. Because of scalability, the diameters of PV generators can vary from some meters up to several hundreds of meters. The output power of a PV generator depends mainly on the irradiance to the PV panels. Therefore, if the irradiance is enhanced, the actual output power might exceed the nominal power. We created a method to estimate the average irradiance over typical land areas of PV generators. The average irradiance over the PV generator land area was used to calculate the frequency, duration and average irradiance of the CE events. The analysis was based on actual irradiance measurement data from an array of pyranometers on an area of 1400 m<sup>2</sup>, which corresponds to the land area of 0.1 MW PV generator. We found out that the focus areas of the CE events have diameters of the order of tens of meters. Therefore, up to 0.1 MW power range, the land area of the PV generator does not greatly affect the maximum average irradiances. In this power range, the average irradiance was measured to be up to 1.5 times the clear-sky irradiance. The CE events affecting utility-scale PV generators were estimated to have maximum average irradiances of 1.4 times the clear-sky irradiance, but the number of these CE events is considerably lower.

## 1. Introduction

The global irradiance is a sum of direct, diffuse and reflected irradiances (Stoffel, 2013). The direct normal irradiance (DNI) is the direct irradiance from the sun on a perpendicular surface to the direct irradiance path, and the diffuse horizontal irradiance (DHI) is the indirect irradiance that is scattered from the clouds, air molecules and aerosols in the atmosphere. The DNI is measured with 2.5° half-angle around the solar disk and therefore, in practice, the direct irradiance contains some diffuse irradiance (Blanc et al., 2014). Reflected irradiances can be caused naturally by snow, water, ice, and ground albedo or by reflections from building facades in built environments. The global tilted irradiance (GTI), i.e., the actual irradiance received by the tilted PV panel depends on its tilt and azimuthal angle, and on several environmental parameters. The nominal power of PV panels is defined under the standard test condition (STC) irradiance of 1000 W/m<sup>2</sup>.

On partly cloudy days, the irradiance can exceed the expected clear sky irradiance value. This well-known phenomenon is known as cloud enhancement (CE), but it is also referred as overirradiance or irradiance enhancement. The CE phenomenon can be observed all around the world – from the equator to high latitudes and from sea level to high altitudes. Measurements of extreme irradiance values have been published on numerous papers. Emck and Richter (2008) measured global

horizontal irradiance (GHI) of 1832 W/m<sup>2</sup> in Ecuador at the altitude of 3400 m, (Gueymard, 2017a) measured GTI of 2000 W/m<sup>2</sup> at 40 degrees Northern latitude at an altitude of 1829 m, and (Yordanov et al., 2015) measured 1.6 kW/m<sup>2</sup> at sea level at 60 degrees of Northern latitude.

Traditionally, the CE phenomenon has been explained by reflections from cloud edges (Norris, 1968). However, this is insufficient and too general explanation of the complex phenomenon. Yordanov et al. (2013a) states that the CE phenomenon is mainly due to strong forward Mie scattering inside the cloud, and that the strongest CE events occur when a narrow gap is surrounded by thin clouds within 5° around the solar disk. In Yordanov et al. (2015), such conditions caused a CE event with irradiance of 1.6 kW/m<sup>2</sup>. Gueymard (2017b) and Gueymard (2017a) reviewed the typical explanations of CE and studied the effect of cloud and albedo enhancement to GHI and GTI. In (Gueymard, 2017b) the CE events were categorized in three groups: (i) the traditional case is the enhancement of irradiance by clouds near the sun disk; (ii) it is possible that under homogenous cloud deck the DHI can be large before and after the CE event so that the cloud edges do not contribute much to the irradiance enhancement, and (iii) the sun is partially obscured by a thin cloud layer so that the DHI can get very high values while the direct irradiance has relatively low values. Especially on cases (ii) and (iii), high ground albedo can further enhance the irradiance. The CE phenomenon has been studied by

\* Corresponding author.

E-mail address: [markku.jarvela@tuni.fi](mailto:markku.jarvela@tuni.fi) (M. Järvelä).

<https://doi.org/10.1016/j.solener.2019.11.090>

Received 22 February 2019; Received in revised form 6 November 2019; Accepted 25 November 2019

0038-092X/© 2019 The Authors. Published by Elsevier Ltd on behalf of International Solar Energy Society. This is an open access article under the CC BY license (<http://creativecommons.org/licenses/by/4.0/>).

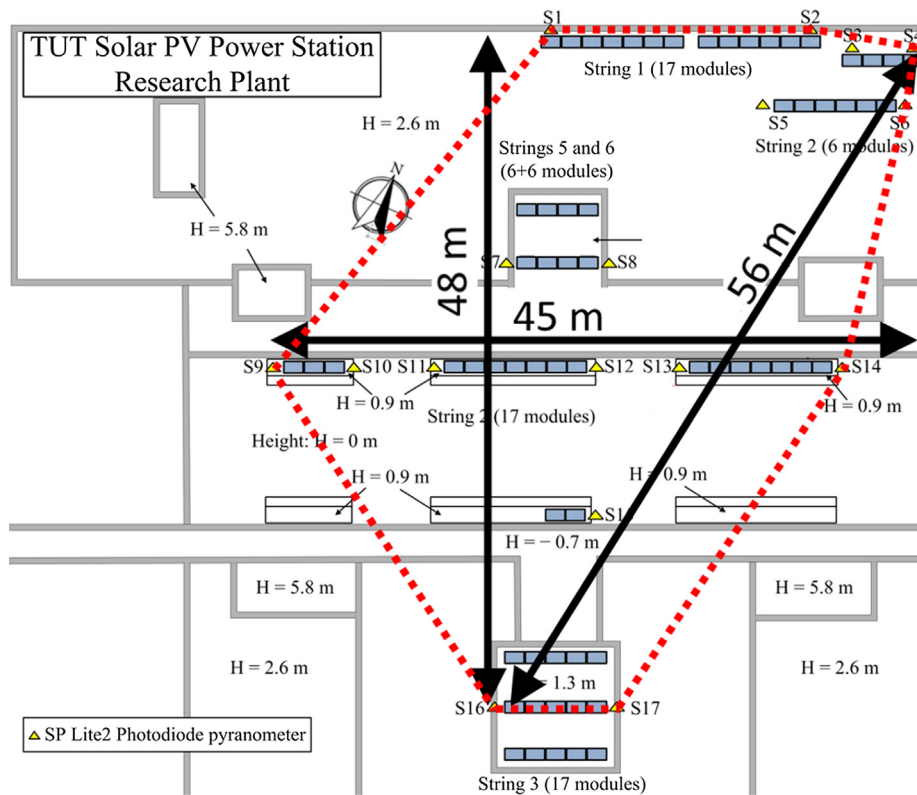


Fig. 1. Dimensions and layout of the TUT solar PV power research plant of Tampere University.

simulations. Yordanov (2015) utilized NASA's I3RC 3D Monte Carlo model to simulate the radiative transfer of solar photons through a gap in a cloud. They showed that in case of overhead sun, irradiance could be 1.8 times the clear-sky irradiance. Pecenek et al. (2016) used 2D Monte Carlo radiative transfer model to study the effect of cloud optical depth and solar zenith angle to the irradiance enhancement. They showed that irradiance could be enhanced 1.47 times the clear-sky irradiance in case of one cloud and 1.63 times in case of two clouds, and that the irradiance enhancement increases with increasing solar zenith angle.

Because the CE phenomenon is tied to clouds, the affected land areas are limited in size. Typically, the irradiance measurements have been done by using only one sensor, and therefore the results cannot be directly applied to large PV generators that are spread on relatively large land areas. If the sampling frequency is too low, the CE events with short duration might not be detected, or similarly, if the response time of the sensor is too long, some CE events might not be detected or several CE events within short time period might be detected as one. Even though the CE phenomenon is well known, its effect on actual PV systems has not been thoroughly studied. Zehner et al. (2012) analyzed the operation of a PV panel during CE events and showed that the power can be 30% higher than the nominal power. The spatial extent of the phenomenon has been covered in some papers. E.g. in Weigl et al. (2012), it was proven that the CE phenomenon can affect the operation of large PV generator by analyzing the irradiance measurement data of 17 pyranometers spread on large land area. Similarly, Espinosa-Gavira et al. (2018) presented a measurement setup consisting of 16 pyranometers spread on land area of  $15\text{ m} \times 15\text{ m}$  with two examples of CE areas covering the test setup completely. However, these papers do not provide systematical analysis on the occurrence or duration of the CE events. Luoma et al. (2012) studied the effect of CE phenomenon on inverter sizing. They estimated the output power of a PV generator by time averaging the irradiance data based on average movement speed of the clouds. In addition, some papers list durations of some of the CE events that can be used to some extent to estimate the land areas of the

CE events (de Andrade and Tiba, 2016; Yordanov et al., 2013a). However, clouds do not move with constant speed (Lappalainen and Valkealahti, 2016) and using an average value does not provide exhaustive results.

The sizes of the CE areas and the average irradiances are relevant factors when assessing the operation of PV power plants. Operational characteristics of PV cells are heavily related to environmental conditions – the short circuit current is almost directly proportional to the irradiance, and the open circuit voltage is inversely proportional to the temperature of the cell. In practice, the irradiance over the PV cell gives a good estimate on what is the maximum output power. Therefore, during the CE events, actual maximum power of a PV generator can be much higher than the nominal power defined in the STC irradiance, especially in cold and in high irradiance environments. If the PV generator power is higher than the rated power of the inverter, the inverter will operate in power limiting mode. In practice, power is limited by increasing the operating voltage, thus reducing the current and consequently the power. The effect of CE events on inverters have been discussed in Tapakis and Charalambides (2014) and on the operating point of the PV generator in Zehner et al. (2012).

The novelty of this paper is in the analysis of average irradiance over land areas corresponding to land areas from residential to large utility-scale PV generators. We studied the characteristics of CE areas by using real irradiance measurement data from an array of pyranometers with sufficient sampling frequency and spatial extent. We created a method to estimate the average irradiance over the land areas of different PV generator sizes and counted the frequency, measured the durations, and calculated the average irradiances of the CE events. The method was validated by comparing the results based on estimated average irradiance to results based on actual average irradiance measured by an array of pyranometers over an area corresponding to a 0.1 MW PV generator and a close accordance was noticed.

## 2. Data

### 2.1. Measurement setup

The measurement data consist of irradiance measurements of 21 photodiode based pyranometers (Kipp & Zonen SP Lite 2) in the TUT solar PV power research plant on the rooftop of Tampere University in Finland in Northern Europe [Torres Lobera et al. \(2013\)](#). The pyranometers have fast response time ( $< 500$  ns to 95%) and they can measure irradiance up to  $2000 \text{ W/m}^2$ . The pyranometers are installed in fixed  $45^\circ$  tilt angle facing  $23^\circ$  east of due south. The irradiance data is read with CompactRIO data-acquisition card by National Instruments, and then stored to database. The dimensions of the research plant and the layout of the panels and pyranometers are presented in [Fig. 1](#). The distance between two furthestmost pyranometers is 56 m and the land area marked with dotted red line is approximately  $1400 \text{ m}^2$ , which corresponds to the land area of a 0.1 MW PV generator ([Ong et al., 2013](#)). This land area consisting of 21 pyranometers is referred later as 0.1 MW TUT PV plant.

### 2.2. Measurement data

The analysis is based on 23 summer months from 2014 to 2018. The sampling frequency of the measurements was 10 Hz. Typically, to ensure the accuracy of the analysis, sub-second sampling frequency is needed when analyzing CE events ([Yordanov et al., 2013b](#)). Irradiance profiles of a clear-sky day on 28th of May 2018 and a partly cloudy day seven days later on 4th of June 2018 are presented in [Fig. 2](#). Both measurements were done with pyranometer S12 located in the middle of the research power plant. Solar noon during these days was 12:22 and 12:23, and sun altitude was  $50^\circ$  and  $51^\circ$ , respectively. Due to the installation angle, the pyranometer is facing the sun at 11:18 and 11:19 while the sun altitude was  $48^\circ$  and  $49^\circ$ , respectively. The peak irradiance value on the clear sky day is approximately  $900 \text{ W/m}^2$ . On average, the clear-sky day peak irradiance measured with this setup in June and July is approximately  $915 \text{ W/m}^2$ . This value is used as reference clear-sky irradiance when analyzing the results. On the partly cloudy day in [Fig. 2](#), irradiance exceeds the clear-sky irradiance numerous times throughout the day. The peak irradiance value was  $1215 \text{ W/m}^2$ , which was 1.32 times the average clear-sky peak irradiance value.

### 2.3. Data validation

Because of the non-ideal measurement environment, occasionally some of the pyranometers were measuring abnormal irradiance values. These abnormalities are caused by small differences in the orientation

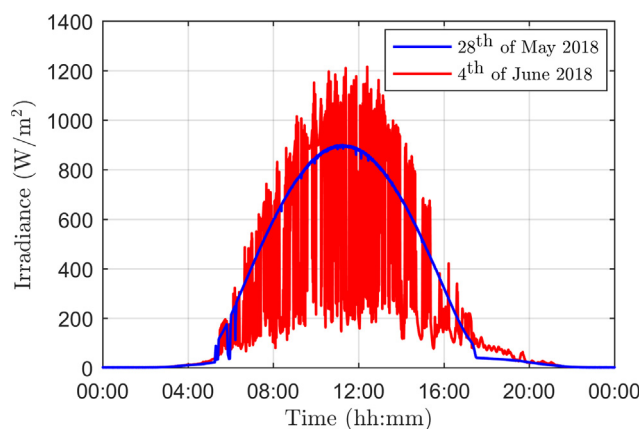


**Fig. 2.** Irradiance profiles on clear-sky and partly cloudy days on 28th of May 2018 and 4th of June 2018.

of the pyranometers, shadings and reflections from the nearby trees and building structures, snow albedo on some spring days, and occasionally some fast shading events are caused by birds. Because of the  $45^\circ$  tilt angle, the pyranometers are susceptible to snow albedo, and therefore inclusion of the days affected by this would unduly skew the results. Therefore, to consider only the effect of the CE phenomenon and to increase the accuracy of the results, we detected these abnormalities by systematically analyzing the clear-sky periods, when all the pyranometers should be under uniform irradiance conditions. In case of some of the measurements had systematic errors, they were fixed to correspond the measurements of other pyranometers. In case the abnormalities were occasional in nature, the measurement data from affected pyranometers was neglected or the day was removed from the analysis. The measurements are affected to some extent by ground albedo during the summer months. The roof is tar-and-gravel roof and the area in front of the pyranometers is mostly open. The  $45^\circ$  tilt angle is close to the typical  $35^\circ$  tilt angle used in Central Europe.

## 3. Methods

### 3.1. Cloud shadow movement

Because the CE events are tied to clouds, the speeds and movement directions of the CE areas can be estimated by analyzing the cloud shadow speeds and movement directions. The cloud shadow speeds and movement directions were calculated by analyzing the time differences of increasing and decreasing irradiance transitions between three nearby pyranometers using the method presented in [Lappalainen and Valkealahti \(2016\)](#). The attenuation of irradiance due to shading with respect to unshaded situation irradiance on the leading and trailing edges of the identified cloud shadows was required to be at least 30%. The irradiance transitions identified in the measured data were parametrized to fit the modified sigmoid function presented in [Lappalainen and Valkealahti \(2015a\)](#). We used pyranometers S2, S5 and S6 to determine the speeds and movement directions of around 18,000 cloud shadows on 512 days. If a different group of sensor had been used, individual speeds and movement directions would have differed slightly, but the average of the speeds would be almost the same ([Lappalainen and Valkealahti, 2015b](#)).

### 3.2. Cloud enhancement area movement

A simple and relatively good method to estimate the movement of CE areas would be to use the daily average speeds of the cloud shadows ([Järvelä et al., 2018](#)). However, on days with clearly changing trend in cloud shadow speeds, the usage of the average speeds will distort the results. To take the variation and changing trends in speeds into consideration, a better method is polynomial curve fitting. [Fig. 3](#) presents a third order polynomial fitting on a day with clear increasing trend of cloud shadow speeds. Because the method used to estimate the cloud shadow speeds is based on assumptions that the cloud shadow edge is linear, the velocity is constant, and the sensors are covered by the shadow of the same cloud, it may occasionally give distinctly odd results to the prevailing trend. Moreover, clouds on several altitudes with different speeds and gusts of wind on the altitude of the clouds may exist which may lead to results differing from the trend. Therefore, 10% of the deviant data points were excluded from the analysis so that the relative root mean square error (RRMSE) of polynomial curve fit was minimized. During the day presented in [Fig. 3](#), the RRMSE of the fit to the speeds of 90% of the cloud shadow event was 13.4% and estimated cloud shadow speeds gradually increased from 9 m/s to 15 m/s.

The estimated speed of cloud shadows matches closely the speed of CE areas. This can be observed in [Fig. 4](#), which presents synchronized irradiance measurements of pyranometer S9 on the west side and S14 on the east side of the research power plant during a CE event on a partly cloudy day on 23rd of May 2015. Both irradiance profiles have

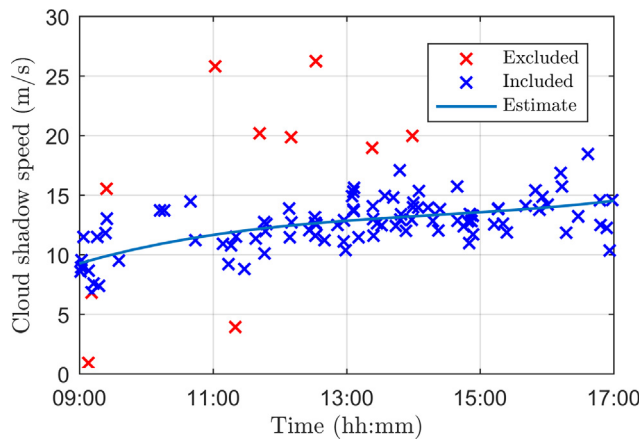


Fig. 3. Cloud shadow speeds and the fitted polynomial curve on 15th of June 2015.

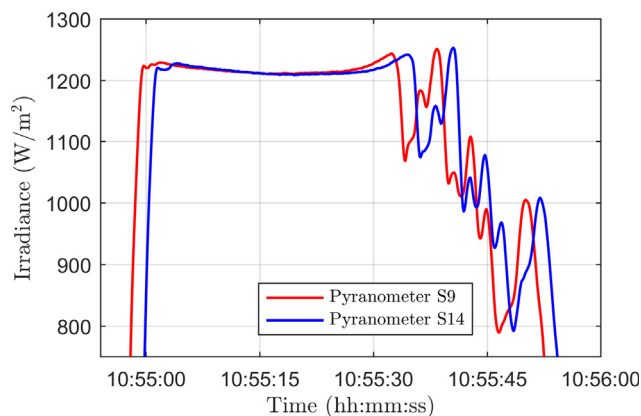


Fig. 4. Synchronized irradiance measurements of two pyranometers 40 m apart from each other on a partly cloudy day on 23th of May 2015.

almost identical shapes. The movement direction of the cloud shadows was approximately from west to east and the speed was about 18 m/s. The time difference between all irradiance transitions is close to two seconds, which matches with the 40 m distance between the pyranometers, and the movement directions and speeds of the cloud shadows. The leading edge of the CE area has smooth transition, but the trailing edge has several fluctuations before the final drop in irradiance. The irradiance peaks at the trailing edge do not have identical values between the pyranometers, meaning that the geometry of the cloud is changing slightly, thus the irradiance is also changing. The duration of the CE event was approximately 33 s when measured from the clean leading edge until the first irradiance dip on the trailing edge. When considering the 18 m/s average movement speed, the diameter of the CE area with almost constant irradiance is more than 0.5 km.

The CE area presented in Fig. 4 was observed on all pyranometers. The leading edge had clean shape and it was perpendicular to the movement direction. The trailing edge did not have as clean shape, but the movement speed was the same as that of the leading edge. Evidently, the CE area edges are tied to clouds and the speeds and movement directions of the CE areas can be deduced by analyzing the speeds and movement directions of the cloud shadows. The irradiance profiles during this CE event are presented in Fig. 10 and further analyzed in Section 4.2.

### 3.3. Validation of the cloud data

When the movement directions and speeds of the cloud shadows are consistent enough, the CE areas are also moving in the same directions,

with the same speeds, and with relatively stable shapes. As presented in Fig. 4, this gives accurate results when calculating the actual diameters of the CE areas. However, it is not always possible to use the average speeds and directions of cloud shadows to estimate the CE area characteristics reliably. Clouds can be categorized into low, mid and high clouds according to their altitude (Houze, 2014) and because of wind shear, wind speed and direction can vary as a function of altitude. Therefore, clouds and consequently cloud shadows can have different movement directions and speeds. In these kinds of cases, the CE areas cannot be presumed to have all the time consistent enough shapes, speeds and movement directions.

The RRMSE gives a good estimate how closely the determined cloud shadow speeds follow the estimated overall speed. Because clouds can be on different layers, the analysis must be limited on days with consistent enough cloud shadow speeds to ensure the affiliation between the cloud shadow and the CE area speeds. The criteria to include the days into the analysis must be strict, because the 10% of the deviant data points, which might have been valid measurements, were removed from the analysis. To get a good estimate of the cloud shadow speeds, we limited the analysis on days with 20 or more identified cloud shadows. In addition, the RRMSE must be under 20% and the estimate of the CE area speed should not change more than 50% of the mean value within a day. The variation in movement directions of cloud shadows within the days was not found to affect the results and therefore it was not used as a validation criterion. The chosen criteria affect directly the accuracy of the results.

We identified cloud shadows on 512 separate days of which 260 had more than 20 identified cloud shadows. The rather strict validation criteria were fulfilled by 77 days. However, seven of these days had to be removed from the analysis because of abnormal irradiance measurements that were too deviant in nature. Eventually, 70 days were included in the final analysis.

### 3.4. Estimating the average irradiance

PV power plants are constructed of blocks consisting of a PV generator, an inverter and a transformer. The power of the PV generator is related closely to the inverter type. Because the PV generator power is almost directly proportional to the land-area, we selected the studied land-areas based on typical power ratings of medium size and large string inverters, and medium size and large central inverters. The powers, land areas, side lengths and power densities of the studied PV generators are listed in Table 1. The land areas are based on typical land areas of such PV generators (Ong et al., 2013). PV generators are assumed to have a square shape, although, in practice, PV generators have different shapes depending on many factors. The side length of the PV generator is used as an input parameter for the simulations. One should also note that the 0.1 MW PV generator with a side length of 35 m corresponds to the land area of the 0.1 MW TUT PV plant, which serves as a reference to validate the results.

To measure the actual irradiances and the shape of the CE areas more precisely, measurements over a huge land area would be required. Unfortunately, such measurements are not available. The average diameter of the cloud shadows is about 800 m and the median diameter is about 300 m (Lappalainen and Valkealahti, 2016). Therefore, we

Table 1

Power ratings, land areas, side lengths, and power densities of the studied PV generators.

Power (MW)	Land area (m <sup>2</sup> )	Side length (m)	Power density (W/m <sup>2</sup> )
0.02	225	15	89
0.1	1225	35	82
1	15,625	125	64
4	62,500	250	64

assumed that the CE areas crossing the PV generators were created by linear cloud edges and the movement direction was perpendicular to the PV generator side with a parallel edge. In this way, the CE areas can be studied in one dimension and calculation of the average irradiance is straightforward. This is a valid assumption when the studied land areas are relatively small. However, the uncertainty of the results increases the larger the studied land-area is. The average irradiance was calculated by time averaging the single point irradiance data. Time averaging factor was calculated based on the side length of the PV generator land area and the estimate of the cloud shadow speed. The average irradiances of the studied PV generator sizes are presented in Fig. 5 for a period of 2 min. The black line presents the raw irradiance data from the pyranometer S12 in the middle of the research power plant and the red line presents the interpolated measured average irradiance over the research power plant area marked with the dashed red<sup>1</sup> line in Fig. 1. The blue, green and magenta lines present the estimated average irradiance over land areas of 0.1, 1 and 4 MW PV generators, respectively. During this period, two CE events occurred, the first lasting approximately 33 s and the second 13 s. The movement speed of the CE areas was 16.5 m/s and, consequently, the diameters of the CE areas were approximately 545 m and 215 m, respectively.

The rate of change of average irradiance depends on the land area of the PV generator. The bigger the land area, the slower are the changes in the average irradiance. In addition, if the diameter of the CE area is smaller than the dimension of the PV generator, the CE area cannot cover the PV generator completely. Consequently, the average irradiance on the PV generator cannot get high values, as is the case with the 4 MW PV generator during the second CE event in Fig. 5.

When the irradiance profile has a clean shape, the estimated average irradiance of the 0.1 MW PV generator and the actual measured average irradiance of the 0.1 MW TUT PV plant matches each other accurately. The biggest differences can be observed during the periods when the irradiance has fast and strong fluctuations or when the edge of the CE area moves over the research power plant. This might cause some inaccuracies in the analysis of CE events with short duration.

### 3.5. Analyzing the cloud enhancement events

An easy way to define a CE event is to compare the average irradiance to clear-sky irradiance value. In there, a CE event begins when the average irradiance exceeds the expected clear-sky irradiance and ends when the irradiance drops below it. However, from the PV power system point of view, a better way is to compare the average irradiance to the STC, clear-sky maximum or some other static irradiance value. Therefore, we recognized all the events where the average irradiance exceeded a certain value. We did this systematically for a range of irradiance values and measured the durations and counted the number of these events for each irradiance value separately. It should be noted, that by using this method, the average irradiance could occasionally drastically exceed the set irradiance limit.

The used definition and analysis of CE events is exemplified in Fig. 6, where the average irradiance of land areas corresponding to 0.1 MW and 4 MW PV generators are aligned with the irradiance data of pyranometer S12. The CE events exceeding a set limit of 1000 W/m<sup>2</sup> are highlighted with a thicker line. The average irradiance of the 0.1 MW PV generator follows the single point irradiance quite closely and, consequently, there are two CE events with durations of 15 s and 19 s. However, under the same irradiance conditions, the average irradiance of the 4 MW PV generator varies less resulting in only one CE event with duration of 29 s, which is due to spatial smoothing. The average irradiance over the 4 MW PV generator stays over the 1000 W/m<sup>2</sup> limit even though there is a brief dip in the measured single point

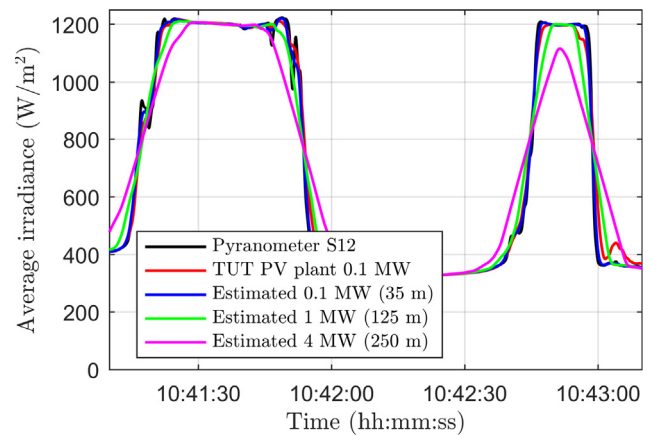


Fig. 5. Average irradiances over the studied PV generator sizes on 27th of July 2015.

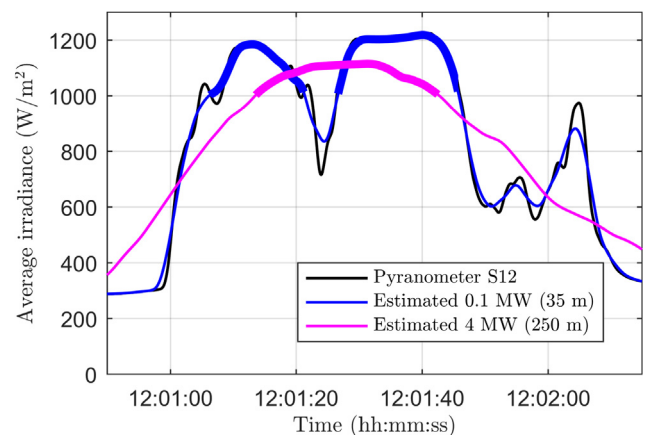


Fig. 6. Irradiance measured with pyranometer S12 and corresponding average irradiances over land areas of 0.1 and 4 MW PV generators on 18th of July 2017.

irradiance. In addition, the peak average irradiance of the 0.1 MW PV generator reaches 1200 W/m<sup>2</sup> but is only 1100 W/m<sup>2</sup> for the 4 MW PV generator.

Durations of the CE events are systematically calculated for different average irradiance limits. It should be emphasized that the average irradiance can considerably exceed the set limit value used to define the beginning and the end of a CE event. This is relevant especially with smaller PV generators where the land areas can be considerably smaller than the CE areas. In addition, the irradiance in some parts of the CE area might also be less than the set limit. This is more relevant for larger PV generators with relatively large land areas.

Average irradiance can be used to estimate the theoretical maximum power of a PV generator. In practice, the actual maximum power of the PV generator depends on several parameters, such as irradiance profile, cell temperature and temperature differences between the cells, configuration and layout of the panels, and movement direction of shading or enhancement areas. The performance of crystalline silicon cells depends heavily on the cell temperature. In steady state conditions, the cell temperature is almost linearly dependent on the irradiance (Koehl et al., 2011). On partly cloudy days the operating conditions can change fast, and the cell temperature can drop during the shading periods preceding the overirradiance events, which will further enhance their effect on the PV generator power. In (Weigl et al., 2012) the operation of a PV power plant during a CE event was simulated when the PV power plant was constructed by either string or central inverters. They showed that the possible non-uniformity of the irradiance profile affects the current–voltage characteristics of the PV

<sup>1</sup> For interpretation of color in Figs. 1, 5, 7, 8 and 12, the reader is referred to the web version of this article.

generator. These non-uniform operation conditions will cause mismatch losses, which will lead to lower actual maximum power than the theoretical maximum power. In Paasch et al. (2014), it was shown that the mismatch losses depend on the movement direction of cloud shadows. However, many of the parameters causing non-homogenous conditions for the PV generator have finally revealed to cause only marginal energy losses. For example, different panel configurations have only a small practical effect on mismatch losses (Lappalainen and Valkealahti, 2017), and instead of one, having multiple maximum power point trackers on spatially long PV string does not affect the net energy gain in long term (Paasch et al., 2015). The inclusion of parameters causing mismatch losses to the simulation model would significantly complicate the analysis and escalate the research space to be infeasible. Therefore, for the sake of clarity, we have chosen to use the simple method of counting the CE events only based on the average irradiance.

#### 4. Results and discussion

##### 4.1. Number of cloud enhancement events

The cumulative number of CE events as a function of average irradiance on PV generators of different sizes are presented in Fig. 7. The number of events decreases with increasing average irradiance and with increasing PV generator land area. In addition, the maximum average irradiance experienced by the PV generators decreases with increasing generator size. The number of CE events experienced by the estimated 0.1 MW PV generator and the actual 0.1 MW TUT PV power plant were almost the same along the analyzed irradiance range.

One main criteria for selecting days for analyses was a minimum of 20 identified shading events in a day. Therefore, the numbers in Fig. 7 cannot be directly used to analyze the overall occurrence of CE events. However, the results can be used to compare the occurrence of the events between PV generators of different sizes. During the 70 days included in the analysis, the irradiance measured with a single pyranometer exceeded the STC irradiance of 1000 W/m<sup>2</sup> approximately 6000 times, and the average irradiance of the 0.1 and 1 MW PV generators exceeded it over 3000 and 2000 times, respectively. The relative difference between the numbers of CE events on 0.1 MW and 1 MW PV generators increases with increasing average irradiance limit. This is plausible due to increase of spatial smoothing of irradiance with increasing generator area.

##### 4.2. Duration of cloud enhancement events

The maximum durations of CE events exceeding the average

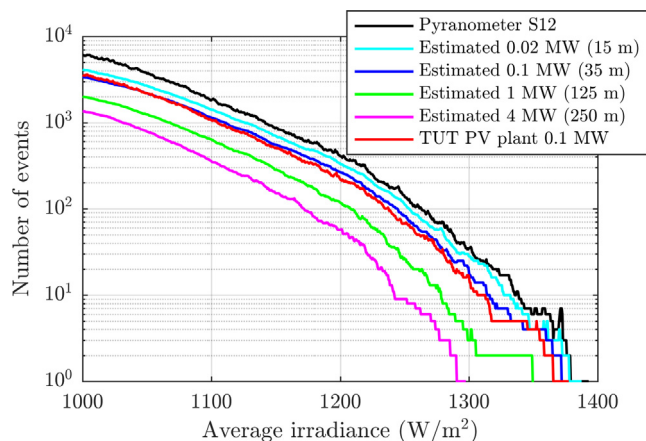


Fig. 7. Cumulative number of CE events as a function of average irradiance on PV generators with different sizes.

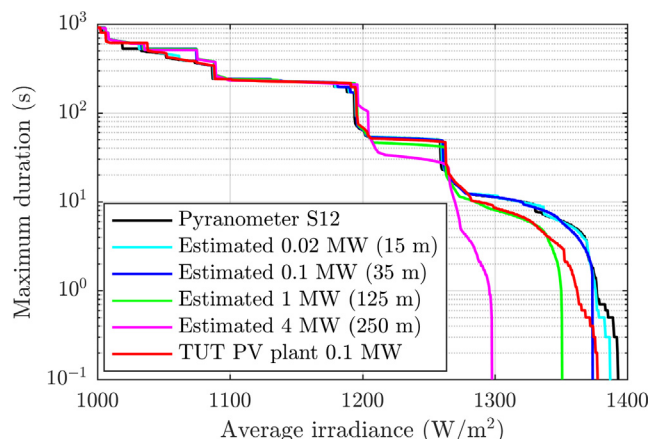


Fig. 8. Maximum durations of CE events exceeding the average irradiance limit of PV generators with different power ratings.

irradiance limit for different PV generator sizes are presented in Fig. 8. The durations of the events decrease fast with increasing irradiance. Peak values of average irradiances were close to 1400 W/m<sup>2</sup>, which is over 1.5 times the average clear-sky peak irradiance. The maximum durations of the strongest CE events with average irradiance exceeding 1300 W/m<sup>2</sup> were approximately ten seconds covering an area with dimensions of few hundred meters. CE events with average irradiances exceeding 1200 and 1100 W/m<sup>2</sup> lasted from one up to four minutes covering areas from several hundred meters up to few kilometers in dimension, respectively. These results are in line with other papers, where the enhanced irradiance has been reported to be over the STC irradiance for several minutes (de Andrade and Tiba, 2016; Yordanov et al., 2013a). The maximum durations of the CE events were not dependent on the PV generator land area up to 1200 W/m<sup>2</sup> irradiance, because the dimensions of PV generators are comparatively small with respect to the diameters of CE areas. Only at high irradiances, the diameters of the CE areas approach the dimensions of PV generators leading to decreasing maximum duration with increasing generator size. The steps in the maximum duration curves are due to single events defining the maximum durations in certain irradiance ranges. For example, the red curve (TUT 0.1 MW) is due to CE events occurring on eight different days.

The maximum durations of the CE events for the estimated 0.1 MW PV generator and for the actual 0.1 MW TUT PV plant are equal almost up to 1300 W/m<sup>2</sup>, but at higher irradiances, the maximum duration on the estimated PV generator is approximately three seconds longer. This is mostly caused by the differences in the dimensions of the actual and estimated PV generators. The 0.1 MW TUT PV plant does not have a square shape and has a long maximum dimension of 56 m compared to the side length of 35 m of the estimated PV generator. Because the measurement setup consists of 21 pyranometers spread on relatively tight grid, it is possible to examine the exact irradiance profiles of the CE events. We used the linear interpolation method of Matlab's griddata function to calculate the irradiance values between the pyranometers. The irradiance profile of a CE event with the peak average irradiance of 1363 W/m<sup>2</sup> is shown in Fig. 9. This event defined the shape of the TUT 0.1 MW maximum duration curve (Fig. 8, red line) on irradiance values of 1282–1363 W/m<sup>2</sup> and for the estimated 0.1 MW area (Fig. 8, blue line) on irradiance values of 1278–1373 W/m<sup>2</sup>. Movement direction of the CE area was approximately from west to east and the speed was 13 m/s. By considering the duration of this CE event (Fig. 8), its diameter can be estimated to be of the order of the side length of the estimated 0.1 MW generator explaining the difference in duration at high irradiances. This is also visible in irradiance distribution of Fig. 9. The extended PV generator areas smooth out these kind of high and fast CE events quite effectively.

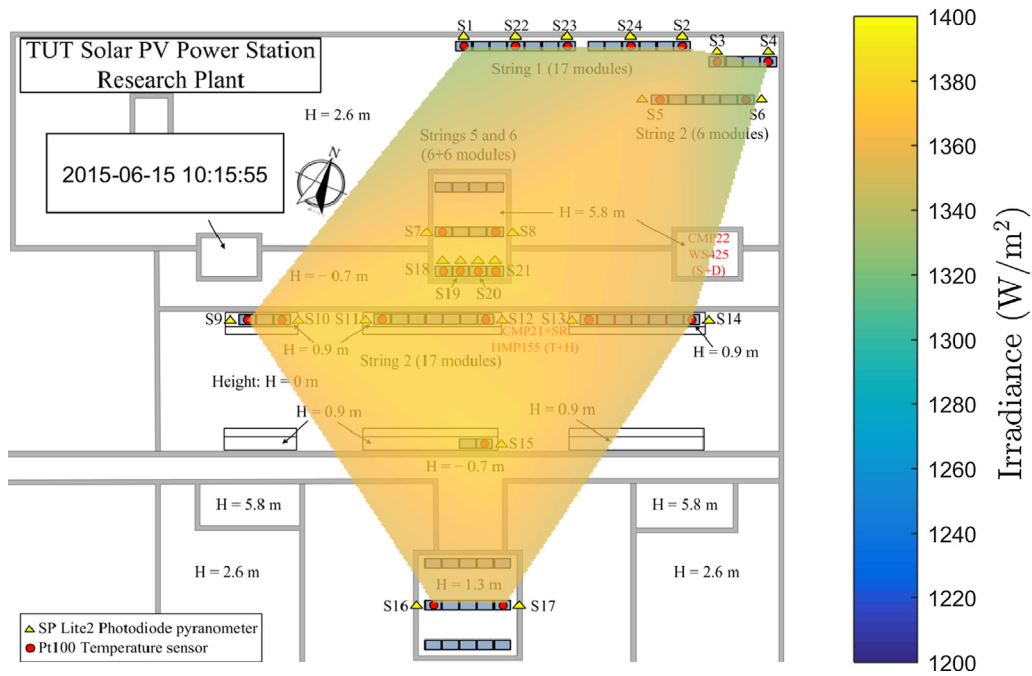


Fig. 9. Irradiance profile of a CE event on 15th of June 2015.

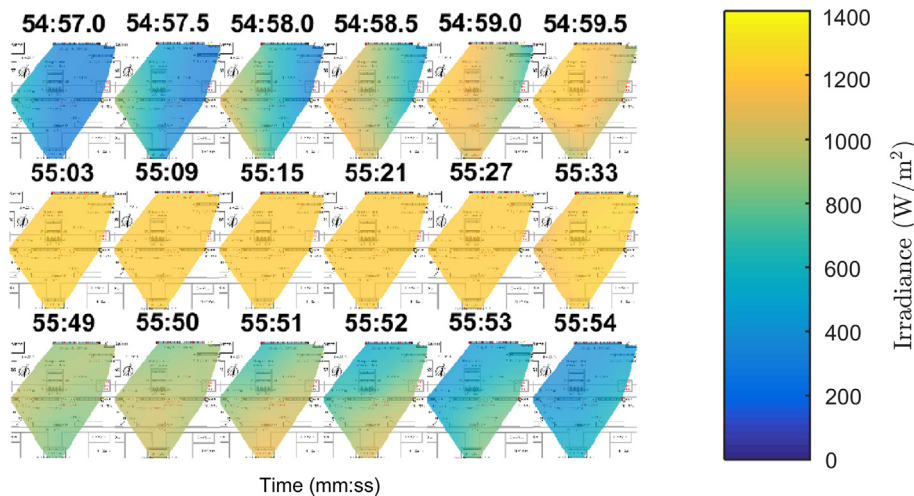


Fig. 10. Irradiance profile of the leading edge (top row), constant irradiance area (middle row) and tailing edge (bottom row) of a CE event on 23th of May 2015.

Because of the 10 Hz sampling frequency, the irradiance data can be used to create detailed videos of the CE area movement. Fig. 10 presents the irradiance profile of the leading edge (0.5 s sampling), constant irradiance area (6.0 s sampling) and the tailing edge (1.0 s sampling) of the CE area presented previously in Fig. 4. The irradiance had clear transition from shaded area to CE area, the edge of the CE area was almost linear, and it was perpendicular to its movement direction. During the CE event, the irradiance remained practically constant. The tailing edge of the CE area did not have a clear transition from CE area to shaded area. However, the movement speed of the tailing edge (leading edge of new cloud shadow), was the same as the leading edge of the CE area (tailing edge of passing cloud shadow).

The maximum durations presented in Fig. 8 are the longest CE events on the observation period. However, the distributions of the durations give a better understanding of typical characteristics of the CE events and their effect on PV power systems. Fig. 11 presents the distributions of the durations of the CE events on the estimated 0.1 MW PV generator and the actual 0.1 MW TUT PV plant for three different irradiance levels. The distributions of the estimates and actual

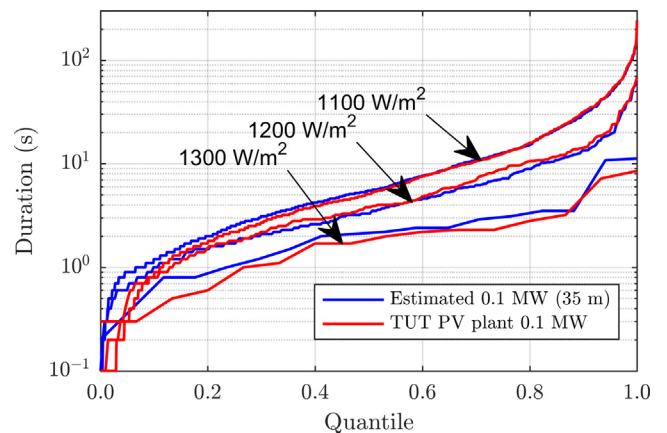
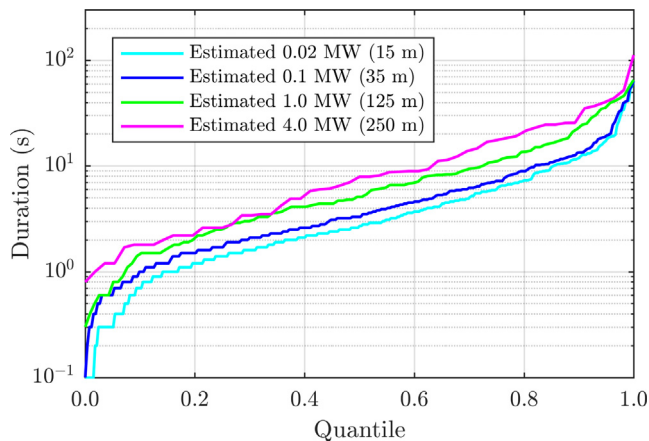


Fig. 11. Distributions of CE event durations exceeding the average irradiances of 1100, 1200 and 1300 W/m<sup>2</sup> over the land areas of the estimated 0.1 MW PV generator and the actual 0.1 MW TUT PV plant.



**Fig. 12.** Distributions of the durations of CE events exceeding  $1200 \text{ W/m}^2$  over the land areas of the estimated 0.02, 0.1, 1 and 4 MW PV generators.

measurements are approximately the same; they differ only at high irradiances to some extent as already discussed in connection of Fig. 8. The distributions have almost the same shape at all irradiance levels, the overall duration just decreases with increasing irradiance enhancement in line with Fig. 8. The share of the CE events with durations exceeding tens of seconds was quite small and the longest measured durations lasting minutes were rare. Similarly, the CE events with durations less than one second were occurring rarely. These events were due to average irradiance peaking at a certain value. Typical duration was from seconds up to a minute having diameters of hundreds of meters. The similarities between the measured and estimated number of the CE events (Fig. 7), maximum duration (Fig. 8), and duration distributions (Fig. 11) validates the used approach for estimating the average irradiance on PV generators.

In Fig. 12 are the distributions of the durations of CE events exceeding the estimated average irradiance of  $1200 \text{ W/m}^2$  over the land areas of the studied PV generators. The shapes of the distribution curves for all the generators are approximately the same as in Fig. 11: the longest and shortest events were quite rare compared to bulk mass of the CE events lasting from seconds up to one minute.

It can be observed from Fig. 8 that the maximum durations were approximately the same for all the PV generator sizes up to average irradiance close to  $1250 \text{ W/m}^2$ . However, the average duration of the CE events increases with increasing PV generator area in Fig. 12. The irradiance profile is the same on all of the PV generators, but due to the spatial smoothing, the peaks and notches are averaged out in large generator areas. Therefore, a sudden but brief drop in irradiance can cause a CE event to be counted as two separate events on a small land area, but as one on large land area leading to longer durations, as exemplified in Fig. 6. Therefore, the number of the CE events and the peak average irradiances increase with decreasing PV generator land area.

## 5. Conclusion

The characteristics of CE events were studied from the PV power generation point of view by analyzing irradiance measurement data from an array of pyranometers spread on land area corresponding to a 0.1 MW PV generator. The irradiance data was used to calculate the speeds and movement directions of cloud shadows. Then the CE area speeds were deduced from the cloud shadow speeds. We also created a simple method to estimate the average irradiances over land areas corresponding to typical PV generator sizes. The method was validated by comparing the estimated average irradiances of CE events to actual measured average irradiances over a land area of a 0.1 MW PV generator. The results obtained by our method matched the actual measurements well. Finally, we calculated the numbers and durations of the

CE events over the land areas of different PV generator sizes.

The average irradiances over land areas up to 0.1 MW PV generator sizes can occasionally be 1.5 times the clear-sky irradiance. Up to this power range, the size of the PV generator does not really affect the expected maximum average irradiance values. This is because the diameters of the strongest CE areas are of the order of tens of meters, which matches the typical dimensions of PV generators in the power range of string inverters. On land areas corresponding to megawatt-scale PV generators, the average irradiances can be over 1.4 times the clear-sky irradiance value. However, the number of the CE events observed by the PV generator decreases with increasing PV generator land area.

The durations of the longest CE events exceeding 1.3 times the clear-sky irradiance were up to several minutes. However, the bulk mass of the events had significantly shorter durations from seconds up to one minute. Because the observed diameters of CE areas can be considerably longer than the dimensions of the PV generators, the PV generator land area does not affect the maximum duration of the events that much. In fact, the larger the PV generator land area is, the longer is the average duration of the CE events. This is because small transitory drops in enhanced irradiance are smoothed out and the average irradiance over large land areas remains at high level.

## Declaration of competing interest

The authors declare that they have no known competing financial interests or personal relationships that could have appeared to influence the work reported in this paper.

## Acknowledgement

This work was funded by Business Finland.

## References

- Blanc, P., Espinar, B., Geuder, N., Gueymard, C., Meyer, R., Pitz-Paal, R., Reinhardt, B., Renné, D., Sengupta, M., Wald, L., Wilbert, S., 2014. Direct normal irradiance related definitions and applications: the circumsolar issue. *Sol. Energy* 110, 561–577. <https://doi.org/10.1016/j.solener.2014.10.001>.
- de Andrade, R.C., Tiba, C., 2016. Extreme global solar irradiance due to cloud enhancement in northeastern Brazil. *Renew. Energy* 86, 1433–1441. <https://doi.org/10.1016/j.renene.2015.09.012>.
- Emck, P., Richter, M., 2008. An upper threshold of enhanced global shortwave irradiance in the troposphere derived from field measurements in tropical mountains. *J. Appl. Meteorol. Climatol.* 47, 2828–2845. <https://doi.org/10.1175/2008JAMC1861.1>.
- Espinosa-Gavira, M.J., Agüera-Pérez, A., de la Rosa, J.J.G., Palomares-Salas, J.C., Sierra-Fernández, J.M., 2018. An on-line low-cost irradiance monitoring network with sub-second sampling adapted to small-scale PV systems. *Sensors* 18, 1–12. <https://doi.org/10.3390/s18103405>.
- Gueymard, C.A., 2017a. Cloud and albedo enhancement impacts on solar irradiance using high-frequency measurements from thermopile and photodiode radiometers. Part 2: Performance of separation and transposition models for global tilted irradiance. *Sol. Energy* 153, 766–779. <https://doi.org/10.1016/j.solener.2017.04.068>.
- Gueymard, C.A., 2017b. Cloud and albedo enhancement impacts on solar irradiance using high-frequency measurements from thermopile and photodiode radiometers. Part 1: Impacts on global horizontal irradiance. *Sol. Energy* 153, 755–765. <https://doi.org/10.1016/j.solener.2017.05.004>.
- Houze, R.A., 2014. Types of clouds in earth's atmosphere. *Int. Geophys.* 3–23. <https://doi.org/10.1016/B978-0-12-374266-7.00001-9>.
- Järvelä, M., Lappalainen, K., Valkealahti, S., 2018. Cloud enhancement phenomenon and its effect on PV generators. In: 35th European Photovoltaic Solar Energy Conference and Exhibition. Brussels, pp. 1964–1968. <https://doi.org/10.4229/35thEUPVSEC20182018-6CV.2.30>.
- Koehl, M., Heck, M., Wiesmeier, S., Wirth, J., 2011. Modeling of the nominal operating cell temperature based on outdoor weathering. *Sol. Energy Mater. Sol. Cells* 95, 1638–1646. <https://doi.org/10.1016/j.solmat.2011.01.020>.
- Lappalainen, K., Valkealahti, S., 2017. Effects of PV array layout, electrical configuration and geographic orientation on mismatch losses caused by moving clouds. *Sol. Energy* 144, 548–555. <https://doi.org/10.1016/j.solener.2017.01.066>.
- Lappalainen, K., Valkealahti, S., 2016. Analysis of shading periods caused by moving clouds. *Sol. Energy* 135, 188–196. <https://doi.org/10.1016/j.solener.2016.05.050>.
- Lappalainen, K., Valkealahti, S., 2015a. Recognition and modelling of irradiance transitions caused by moving clouds. *Sol. Energy* 112, 55–67. <https://doi.org/10.1016/j.solener.2014.11.018>.
- Lappalainen, K., Valkealahti, S., 2015b. Recognition of shading events caused by moving

- clouds and determination of shadow velocity from solar radiation measurements. In: 31st European Photovoltaic Solar Energy Conference and Exhibition, pp. 1568–1573. <https://doi.org/10.4229/EUPVSEC20152015-5AO.7.5>.
- Luoma, J., Kleissl, J., Murray, K., 2012. Optimal inverter sizing considering cloud enhancement. *Sol. Energy* 86 (1), 421–429. <https://doi.org/10.1016/j.solener.2011.10.012>.
- Norris, D.J., 1968. Correlation of solar radiation with clouds. *Sol. Energy* 12, 107–112. [https://doi.org/10.1016/0038-092X\(68\)90029-7](https://doi.org/10.1016/0038-092X(68)90029-7).
- Ong, S., Campbell, C., Denholm, P., Margolis, R., Heath, G., 2013. Land-Use Requirements for Solar Power Plants in the United States. Golden, CO (United States). <https://doi.org/10.2172/1086349>.
- Paasch, K.M., Nymand, M., Kjaer, S.B., 2014. Simulation of the impact of moving clouds on large scale PV-plants. 2014 IEEE 40th Photovolt Spec. Conf. PVSC 2014, pp. 791–796 <https://doi.org/10.1109/PVSC.2014.6925036>.
- Paasch, K.M., Nymand, M., Kjar, S.B., 2015. Long term energy yield measurements of a string- vs. central inverter concept tested on a large scale PV-plant. 2015 17th Eur. Conf. Power Electron. Appl. EPE-ECCE Eur. 2015. <https://doi.org/10.1109/EPE.2015.7311679>.
- Pecenak, Z.K., Mejia, F.A., Kurtz, B., Evan, A., Kleissl, J., 2016. Simulating irradiance enhancement dependence on cloud optical depth and solar zenith angle. *Sol. Energy* 136, 675–681. <https://doi.org/10.1016/j.solener.2016.07.045>.
- Stoffel, T., 2013. Terms and definitions. In: *Solar Energy Forecasting and Resource Assessment*. Elsevier, pp. 1–19. <https://doi.org/10.1016/B978-0-12-397177-7.00001-2>.
- Tapakis, R., Charalambides, A.G., 2014. Enhanced values of global irradiance due to the presence of clouds in Eastern Mediterranean. *Renew. Energy* 62, 459–467. <https://doi.org/10.1016/j.renene.2013.08.001>.
- Torres Lobera, D., Mäki, A., Huusari, J., Lappalainen, K., Suntio, T., Valkealahti, S., 2013. Operation of TUT solar pv power station research plant under partial shading caused by snow and buildings. *Int. J. Photoenergy*. <https://doi.org/10.1155/2013/837310>.
- Weigl, T., Nagl, L., Weizenbeck, J., Zehner, M., Augel, M., Öchsner, P., Giesler, B., Becker, G., Mayer, O., Betts, T., Gottschalg, R., 2012. Modelling and validation of spatial irradiance characteristics for localised irradiance fluctuations and enhancements. In: 27th European Photovoltaic Solar Energy Conference and Exhibition, pp. 3801–3804. <https://doi.org/10.4229/27thEUPVSEC2012-5CO.7.6>.
- Yordanov, G.H., 2015. A study of extreme overirradiance events for solar energy applications using NASA's I3RC Monte Carlo radiative transfer model. *Sol. Energy* 122, 954–965. <https://doi.org/10.1016/j.solener.2015.10.014>.
- Yordanov, G.H., Midtgård, O.-M., Saetre, T.O., Nielsen, H.K., Norum, L.E., 2013a. Overirradiance (cloud enhancement) events at high latitudes. *IEEE J. Photovoltaics* 3, 271–277. <https://doi.org/10.1109/JPHOTOV.2012.2213581>.
- Yordanov, G.H., Saetre, T.O., Midtgård, O.-M., 2013b. 100-millisecond Resolution for accurate overirradiance measurements. *IEEE J. Photovoltaics* 3, 1354–1360. <https://doi.org/10.1109/JPHOTOV.2013.2264621>.
- Yordanov, G.H., Saetre, T.O., Midtgård, O.M., 2015. Extreme overirradiance events in Norway: 1.6 suns measured close to 60°N. *Sol. Energy* 115, 68–73. <https://doi.org/10.1016/j.solener.2015.02.020>.
- Zehner, M., Weigl, T., Thaler, S., Schrank, O., Czakalla, M., Mayer, B., Betts, T.R., Gottschalg, R., Behrens, K., Langlo, G.K., Giesler, B., Becker, G., Mayer, O., 2012. Energy loss due to irradiance enhancement. In: 26th European Photovoltaic Solar Energy Conference and Exhibition, pp. 3935–3938. <https://doi.org/10.4229/26thEUPVSEC2011-5AO.6.3>.